Two Pore Types in the Inner-Wall Endothelium of Schlemm's Canal

C. Ross Ethier,[1] Fides M. Coloma,[1] Arthur J. Sit,[2] and Mark Johnson[2]

Purpose. It has been reported that fixation conditions significantly influence the apparent pore density in the inner-wall endothelium of Schlemm's canal. In the present study, the manner in which fixation conditions affect the two subtypes of inner-wall pores, intracellular pores and intercellular (or border) pores, was investigated.

Methods. Outflow facility was measured in enucleated human eyes. Eyes were fixed under "constant flow" or constant pressure conditions, microdissected to expose the inner wall of Schlemm's canal, and prepared for scanning electron microscopy. The density and diameter of the two subtypes of pores in the inner wall were measured.

Results. Intracellular pore density decreased with increasing postmortem time ($P < 0.001$) and increased with increasing volume of fixative passed through the outflow pathway ($P < 0.001$), whereas border pore density showed no dependence on these parameters ($P > 0.25$ and $P > 0.15$, respectively). Border pore density increased with increasing fixation pressure ($P < 0.005$), even though intracellular pore density showed no such dependence ($P > 0.4$). No correlation was found between outflow facility and the predictions of Poiseuille's law, Sampson's law, or the funneling theory for the hydraulic conductivity of the intracellular pores ($P > 0.35$) or the border pores ($P > 0.1$).

Conclusions. The intracellular and border pores form two morphologically and functionally distinct populations in the inner wall of Schlemm's canal. The dependence of intracellular pore density on postmortem time and on volume of fixative passed through the outflow pathway suggests that these pores are artifacts of tissue fixation or processing conditions. That border pores do not depend on such conditions and that their presence is correlative with perfusion pressure suggests that this population may be nonartifactual. New histologic techniques for examining the inner wall of Schlemm's canal are necessary to determine the in vivo state of inner-wall pores and how they influence outflow facility. (*Invest Ophthalmol Vis Sci.* 1998;39:2041-2048)

The cause of the elevated aqueous humor outflow resistance characteristic of primary open-angle glaucoma[1] is unknown. Among the difficulties in localizing the pathologic condition responsible for outflow obstruction is the inability to determine the locus of outflow resistance, even in healthy eyes. An early[2] candidate site for generating aqueous outflow resistance has been the inner wall of Schlemm's canal. When eyes are fixed at pressure, it has been observed that the inner wall of Schlemm's canal contains giant vacuoles protruding from the endothelial layer into the lumen of Schlemm's canal.[3-5] Associated with these giant vacuoles but also occurring in other areas[6] are pores passing through the inner wall. However, the pioneering hydrodynamic studies of Bill and Svedbergh[7] and confirmation of their results by other investigators[8,9] showed that the inner-wall pores could be responsible for, at most, a modest fraction of total outflow resistance. Simply put, there were just too many holes in the inner-wall endothelium.

Since that time, investigations have focused on the possibility that the juxtacanalicular connective tissue, and in particular, its extracellular matrix, generates the bulk of aqueous outflow resistance.[10-12] Experimental evidence has confirmed that a significant fraction of outflow resistance is generated by the juxtacanalicular connective tissue.[13] However, this result leaves unexplained the experimental observations[14,15] that an increase in the pore density of the inner-wall endothelium is associated with an increase of outflow facility and that return of the pore density to its baseline value is associated with rapid restoration of outflow facility.

Using perfusion studies in combination with scanning electron microscopy (EM), we have recently found that the density of pores in the inner-wall endothelium depends on fixation conditions.[16] Specifically, in fresh human eyes (perfused less than 20 hours after death) total pore density in-

From the [1]Department of Mechanical Engineering and Ophthalmology, University of Toronto, Canada; and the [2]Department of Mechanical Engineering, Massachusetts Institute of Technology, Cambridge.

Supported in part by Grant EY09699 from the National Institutes of Health, Bethesda, Maryland; Grant MA-10051 from the Medical Research Council of Canada, Ottawa, Ontario, Canada, and the Natural Sciences and Engineering Research Council of Canada, Ottawa, Ontario, Canada (partial support for AJS).

Presented in part at the annual meeting of the Association of Research in Vision and Ophthalmology, Fort Lauderdale, Florida, May 1997.

Submitted for publication February 12, 1997; revised June 20, 1997; accepted July 9, 1998. The delay in publication was caused by an oversight during the editorial transition.

Proprietary interest category: N.

Reprint requests: C. Ross Ethier, Department of Mechanical and Industrial Engineering, University of Toronto, 5 King's College Road, Toronto, Ontario, M5S 3G8 Canada.

Copyright © Association for Research in Vision and Ophthalmology

creased with the total volume of fixative that passed through the inner wall. This suggests that the in vivo state of the inner-wall pores may differ from that seen in fixed specimens and thus potentially reopens questions about the role (if any) that the inner wall plays in influencing aqueous outflow resistance.

During the course of the previous study [16], we observed two distinct pore types in the inner-wall endothelium of Schlemm's canal: pores passing through cells (intracellular pores) and pores passing between cells (intercellular or "border" pores). The latter type of pore is consistent with observations of a paracellular pathway for aqueous humor drainage, described by Epstein and Rohen.[17]

The goal of the present study was to characterize more completely these two types of pores in the inner-wall endothelium. In particular, in view of our previous work showing fixation-induced changes in pore density, we sought to determine what effect perfusion and fixation conditions had on each type of pore. This was achieved by examining the inner-wall endothelium of eyes perfused and fixed under a variety of conditions, including constant-flow fixation.

Methods

Most of the experimental methods used in the present study were identical with those previously reported,[16] and therefore will be summarized only briefly here. The same two series of postmortem normal human eyes were used in the present study as were used in our previous work. The measured parameters for each eye are defined in Table 1 and summarized in Table 2.

Eyes were excluded if donors had had ophthalmic surgery, diabetes, or a history of ocular disease. In series A, 21 eyes (10 pairs plus a single eye) were perfused with Dulbecco's phosphate-buffered saline (Life Technologies, Grand Island, NY) with 5.5 mM glucose added at a constant flow rate of 2 μl/min, and were then subjected to anterior chamber exchange and fixation under constant-flow conditions. More specifically, anterior chamber exchange and fixation using modified Karnovsky's fluid (2.5% glutaraldehyde and 2% paraformaldehyde in Sörenson's phosphate buffer [pH 7.3]) was carefully performed at the constant pressure recorded at the end of the conventional perfusion, that is, just before anterior chamber exchange. This produced approximately equal fixation flow rates (but different pressures) in all eyes. In series B, 13 eyes were perfused at a constant pressure of 8 mm Hg and were then subjected to anterior chamber exchange. In 8 of the 13 eyes, subsequent constant pressure fixation was performed at 8 mm Hg; in the remaining 5 eyes, the fixations were performed at an elevated pressure that was constant during the fixation procedure (range, 9-46 mm Hg).

At the conclusion of fixation, the inner wall of Schlemm's canal was prepared for scanning EM, and pore densities and diameters were analyzed using previously described methods.[16] Briefly, probable pores were identified from montages, and the original samples were then rescanned at magnification ×10,000 to verify that each putative pore was nonartifactual. Openings in the endothelium were identified as artifactual tears and disregarded if the edges were rough, torn, irregular, or notched. Border pores were defined to be those pores observed by scanning EM to intersect with a cell margin, whereas intracellular pores were those pores that did not intersect a cell margin. A small percentage of the pores (2%-3%) could not be definitively classified and were not included in either category. A typical image of the inner-wall endothelium with the two pore types identified (intracellular and border) is shown in (Figure 1); note the irregular margins of the artifactual pore.

Table 1. Nomenclature for Parameters Measured in the Present Study

Measured Quantity	Symbol	Units
Patient age	Age	years
Postmortem time to the start of the experiment	PM	hours
Time between patient death and enucleation	E	hours
Intracellular pore density of the inner wall endothelium	N_I	pores/mm^2
Border pore density	N_B	pores/mm^2
Average intracellular pore diameter	D_I	μm
Average border pore diameter	D_B	μm
Outflow facility before fixation	C	μl/min/mm Hg
Outflow facility after fixation (series A only)	C_F	μl/min/mm Hg
Fixation pressure	IOP	mm Hg
Flow rate of buffer through outflow pathway before fixation	Q	μl/min
Volume of buffer perfused through outflow system before fixation	V_B	ml
Volume of fixative perfused through outflow system (series A only)	V_F	ml
Time that fixative was perfused through the outflow system	T	min

Because pores are typically elliptical, the major and minor axes were measured directly from the screen of the microscope at ×10,000. Length measurements were calibrated using two scanning EM calibration grids (SIRA Institute, Chislehurst, England) with densities of 19.7 lines/mm and 2160 lines/mm. Because circular pores will appear elliptical when viewed in tilted section, the pore diameter was assumed to be equal to the major axis of the pore; however, all results reported in this article were also verified using the geometric mean of the major and minor axes as the pore diameter.

Statistical Methods and Quantitative Analysis

The measured parameters for each eye included patient age (Age: in years), postmortem time to the start of the experiment (PM: in hours), time between patient death and enucleation (E: hours), intracellular pore density of the inner-wall endothelium (N_I: pores per square millimeter), border pore density (N_B: pores per square millimeter), average intracellular pore diameter (D_I: in micrometers), average border pore diameter (D_B: in micrometers), outflow facility before fixation (C: in microliters

TABLE 2. Summary of Experimental Data for Each Eye

Eye	Age (y)	PM (h)	IOP (mm Hg)	C (μl/min/mm Hg)	C_F (μl/min/mm Hg)	N (pores/mm^2)			D (μm)			T (min)	V_F (ml)
						I	B	Total	I	B	Total		
Q5	86	14.33	43	0.050	0.025	753.6	613.3	1417.8	0.95	1.69	1.31	115	0.115
Q6	86	14.33	41	0.050	0.030	1255.2	614.0	2014.2	1.34	1.72	1.52	115	0.138
Q7	71	25.83	11.8	0.170	0.080	1060.0	394.5	1485.4	0.81	1.39	0.97	338	0.318
Q8	71	25.83	9.4	0.210	0.110	2263.6	620.1	2935.7	1.13	1.85	1.32	338	0.355
Q9	5	24.75	2.9	0.700	0.400	1236.5	1305.5	2542.0	0.82	1.39	1.11	460	0.524
Q10	5	24.75	3.1	0.650	0.750	1063.1	478.4	1562.8	0.84	1.44	1.02	134	0.310
Q13	97	13.43	18.6	0.110	0.050	2234.8	622.8	2958.3	1.02	1.70	1.20	283	0.258
Q14	97	13.43	25.5	0.080	0.045	893.0	284.9	1275.1	0.81	1.54	1.03	93	0.105
Q15	62	34.3	10.2	0.195	0.065	259.5	363.3	622.9	1.36	1.45	1.41	98	0.066
Q16	62	34.3	10.5	0.190	0.120	161.7	452.9	614.6	1.08	1.44	1.34	258	0.325
Q17	93	17.8	28.7	0.070	0.045	620.2	772.8	1446.6	0.87	1.24	1.09	62	0.08
Q18	93	17.8	21.4	0.090	0.053	1210.9	341.0	1563.1	0.74	1.48	0.91	240	0.283
Q19	65	8.33	10.2	0.200	0.080	2166.8	493.0	2670.8	0.79	1.14	0.86	270	0.283
Q20	65	8.33	8.3	0.240	0.110	1698.6	369.2	2091.4	0.97	1.58	1.08	93	0.098
Q21	50	27.98	3.5	0.640	0.275	55.3	118.2	173.5	1.63	2.36	2.13	706	0.725
Q23	85	26.98	4.4	0.425	0.131	136.4	60.2	211.5	1.21	2.64	1.65	506	0.363
Q24	85	26.98	7.5	0.268	0.075	798.9	130.3	960.2	0.88	1.67	1.03	181	0.114
Q25	91	10.58	17.2	0.115	0.035	1458.4	234.9	1704.8	1.24	1.71	1.31	180	0.149
Q26	91	10.58	21.9	0.090	0.035	1612.1	204.3	1838.0	1.29	1.52	1.33	181	0.170
Q27	75	20.25	15.1	0.130	0.080	750.5	205.6	961.2	0.92	1.11	0.97	75	0.091
Q28	75	20.25	9.4	0.210	0.070	410.1	377.3	791.5	0.96	1.64	1.28	345	0.272
258	85	25	9	0.34		834.1	419.4	1279.6	0.95	1.76	1.24	120	
262	79	34	46	0.07		465.3	487.6	988.6	1.02	1.60	1.34	150	
264	75	27	25	0.15		1277.2	470.3	1804.1	0.74	1.89	1.05	60	
270	74	23	8	0.26		456.2	199.5	686.8	0.87	1.45	1.08	120	
274	85	25	27	0.08		660.9	360.4	1042.7	0.91	1.88	1.27	100	
276	87	17	19	0.12		149.3	68.6	230.8	1.10	1.98	1.36	60	
242	86	31	8	0.18		724.6	140.1	864.7	0.74	1.59	0.87	60	
244	77	27	8	0.05		105.1	36.2	149.8	0.54	1.96	0.90	60	
246	90	25	8	0.17		883.4	177.0	1060.3	1.21	2.53	1.43	60	
250	81	27	8	0.14		800.9	274.2	1105.1	0.78	1.18	0.89	90	
251	85	13	8	0.19		857.5	283.2	1140.8	0.70	1.17	0.82	60	
268	84	19	8	0.17		473.7	163.6	643.9	0.87	1.57	1.06	130	
282	76	18	8	0.12		838.4	138.6	990.0	0.99	1.67	1.10	90	

See Table 1 for definition of symbols. Blank cells indicate that no data were measured.

per minute per millimeter of mercury), outflow facility after fixation (C_F: microliters per minute per millimeter of mercury; series A only), fixation pressure (IOP: in millimeters of mercury), flow rate of buffer through outflow pathway before fixation (Q: in microliters per minute), volume of buffer perfused through outflow system before fixation (V_B: in milliliters), volume of fixative perfused through outflow system (V_F: in milliliters; series A only), and time that fixative was perfused through the outflow system (T: in minutes) (Table 2).

We also included one derived parameter in the data analyses. Because we did not measure V_F in series B, we defined a new parameter V_F' (in milliliters) = $0.5 \cdot Q \cdot T$, which is an estimate of the volume of fixative perfused through the outflow system based on the observation that outflow facility rapidly decreases by 50% during fixation[16]. Because V_F, V_F', and T were closely related and thus not statistically independent, we used only one of these parameters in any regression analysis. If one of these parameters yielded a statistically significant correlation, all were investigated to determine which produced the lowest P.

We first performed linear regression analyses relating outflow facility to pore density and pore density to fixation flow rate and fixation pressure. We then performed multivariate regression analyses (Systat for Macintosh, version 5.2.1; SPSS, Chicago, IL) examining the correlation of three of the variables (outflow facility, pore density, and pore diameter) with the remaining variables measured in series A and B. Variables that were not plausibly connected to the dependent variable were not included in the correlation (e.g., fixation time could not affect prefixation outflow facility), nor were variables that could be directly used to calculate the dependent variable (e.g., flow rate and pressure were not both included in correlations for outflow facility). We used an automated forward stepwise regression as implemented in the software (Systat) using a tolerance (overall P) of 0.01 and P for adding variables to the correlation of 0.01. In this scheme, at each step of the iteration, the most statistically significant variable not yet included in the correlation was added to the correlation while ensuring that the tolerance did not exceed 0.01. The most statistically significant variable was chosen by computing which of the remaining variables not yet added to the correlation would have the lowest individual P (constrained to be less than 0.01) if it were added to the correlation. When no further variables could be added without having the tolerance exceed

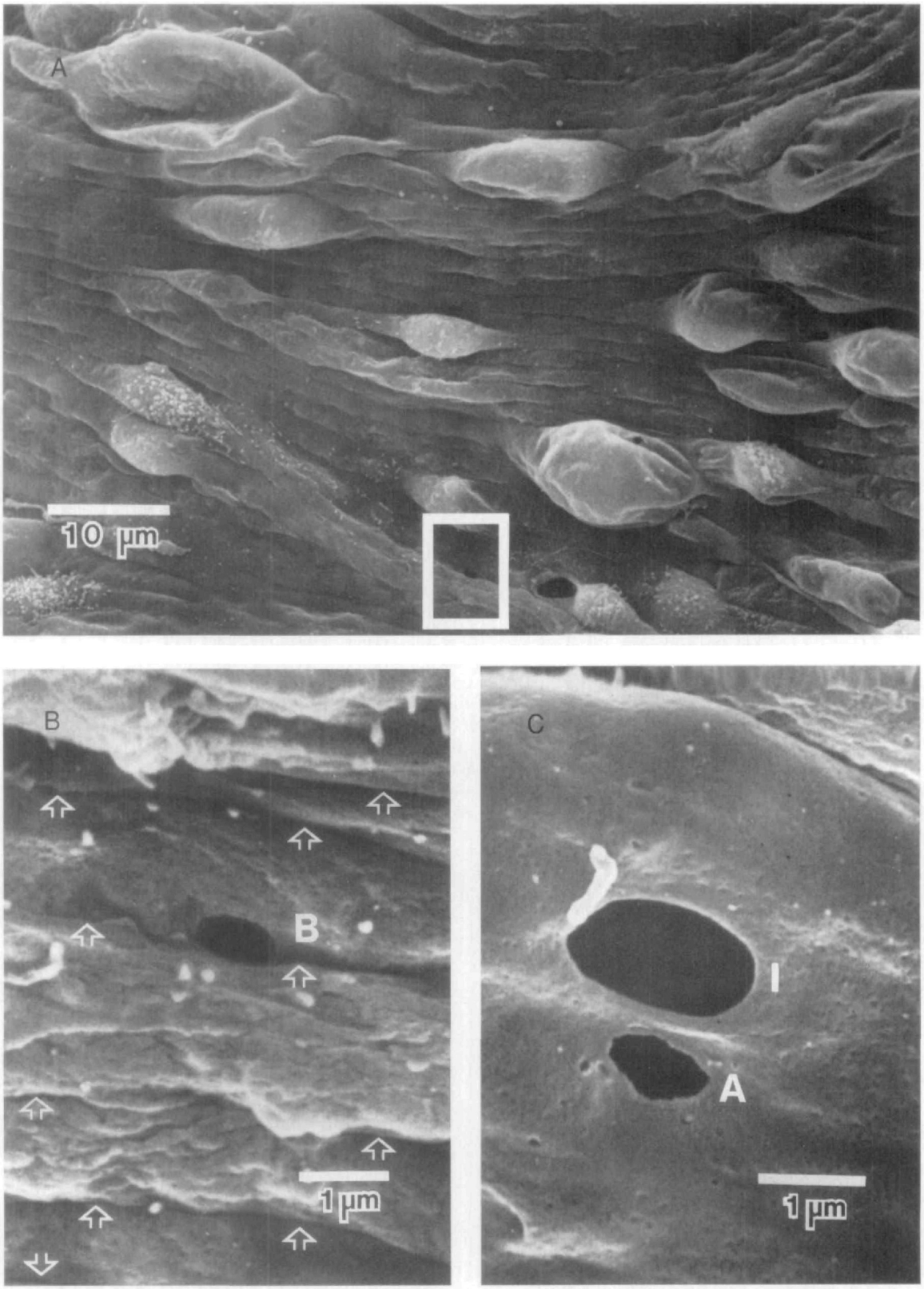

Figure 1. Scanning electron photomicrographs of pores in inner-wall endothelium. (**A**) Overview of section of inner wall. (**B**) High-power view of intercellular or border pore (**B**) from boxed region in (**A**). (**C**) High-power view of intracellular pore I and artifactual pore A. *Arrows* in (**B**) refer to cellular margins. Note that the (**B**) pore is intersected by a cellular margin on each edge. An overview micrograph of the region that contains (**C**) was published in reference 16. Scale bar, (**A**) 10 μm; (**B**, **C**) 1 μm.

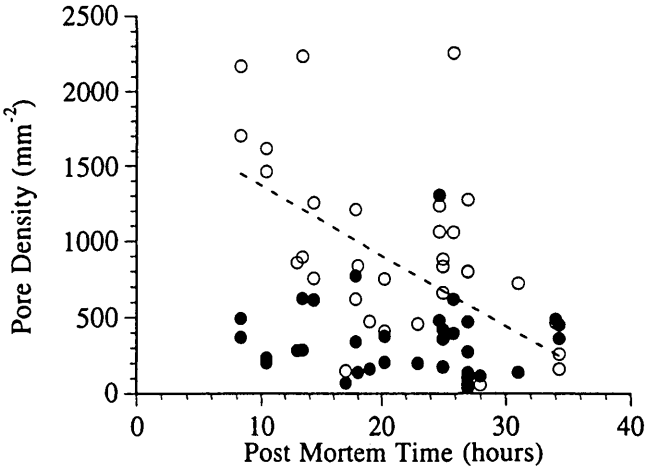

FIGURE 2. Pore density as a function of postmortem time. (○), intracellular pores; (●), border pores. *Dashed line* is best linear fit to intracellular pore data ($P < 0.001$). No correlation was found between border pore density and postmortem time ($P > 0.25$).

0.01, the iteration was terminated, giving both an overall P for the correlation and individual P to each of the correlated variables.

The residuals (the difference between the fitted value of the dependent parameter and its measured value) were examined and in all cases seemed random when plotted against the independent variables. Outliers from the fit and points with high leverage, identified by the software program, were also examined. If the externalized Studentized residual (analogous to a t-statistic) had a probability of occurrence less than $0.01/N$ (where N is the number of data points), this point was removed from the fit.[18] Points with high leverage with a Cook distance greater than 1 were also removed.[18] A single point was found to be an outlier and have high leverage by these criteria, and it is noted in the Results section.

We also examined correlations between the two types of pores. Specifically, we determined (Systat) the Pearson correlation coefficient (r) and its statistical significance comparing the pore density and pore diameters of the intracellular and border pores.

Unless otherwise stated, combined data from series A and B were used in all statistical analyses. Because our previous study[16] indicated that pore density was affected by postmortem time, we were concerned that this correlation might mask other correlations, and we therefore performed statistical analyses not only on the entire data set, but also on three subsets of the data: eyes on which experimentation had begun within 15, 20, or 25 hours after death.

Both eyes from series A were used initially as independent data points, because in most pairs one eye had a lower fixation time at flow and was perfused with less fixative volume than was the contralateral eye. However, to account for the nonindependence of the two eyes of a pair,[19] we reanalyzed the data using two methods, as previously described.[16] In no case did these corrections yield $P > 0.05$ in any case found to be statistically significant, and thus only P calculated assuming each eye to be statistically independent is reported below. P reported is from two-tailed Student's t-test.

RESULTS

Pore Densities

Strikingly different statistics were found for the two types of pores. We found that N_I decreased with increasing PM (Fig. 2) and increased with increasing volume of fixative perfused (V_F') (Fig. 3).

$$N_I = a_0 + a_1{*}\mathrm{PM} + a_2{*}V_F' \quad (1)$$

with coefficients and significance levels as shown in Table 3. Using V_F for series A and V_F' for series B yielded correlations similar to those in Eq. 1. If instead of V_F', T was used in the correlation, we found that

$$N_I = b_0 + b_1{*}\mathrm{PM} + b_2{*}T \quad (2)$$

with the coefficients and significance levels shown in Table 4.

Turning next to the intercellular or border pores, we found that one eye had a much higher density of border pores (N_B = 1306 pores/mm^2; Age = 5 years, PM = 24.75 hours; E = 1.6 hours) than did the other eyes, and was excluded as an outlier based on the criteria described in the Methods section (Fig. 4). In the remaining eyes, we found that border pore density correlated only with the perfusion pressure:

$$N_B = c_0 + c_1{*}\mathrm{IOP} \quad (3)$$

with the coefficients and significance levels shown in Table 5. This finding is in contradistinction to the finding with N_I, which showed no correlation with IOP ($P > 0.4$). The difference in characteristics between N_B and N_I is emphasized by noting that both V_F' and PM, two parameters strongly correlated with N_I, were not correlated with N_B ($P > 0.15$ and $P > 0.25$, respectively).

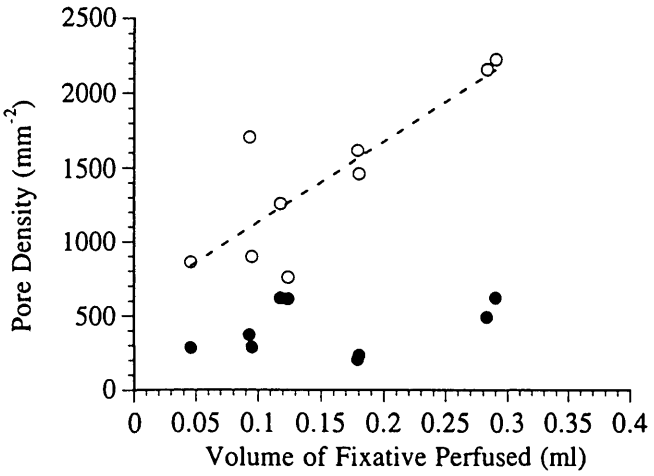

FIGURE 3. Pore density as a function of volume of fixative perfused through outflow pathway for eyes with postmortem time less than 15 hours. (○), intracellular pores; (●), border pores. The *dashed line* is the best linear fit to the intracellular pore data (Eq. 1; $P < 0.005$). No correlation was found between border pore density and volume of fixative perfused ($P > 0.15$).

TABLE 3. Coefficients for Equation 1

Postmortem Time (h)	n	a_0	a_1	a_2	P^*
All data	34	1830 ± 270	−43.2 ($P < 0.001$)	NS ($P = 0.44$)	<0.001
<25 hours	19	1870 ± 320	−75.9 ($P < 0.001$)	2630 ($P < 0.005$)	<0.001
<20 hours	14	1710 ± 400	−82.9 ($P < 0.005$)	4450 ($P < 0.001$)	<0.00005
<15 hours	9	580 ± 230	NS ($P = 0.078$)	5450 ($P < 0.005$)	<0.005

NS, not significant at $P = 0.01$. Values for a_0 are means ± SE and means for a_1 and a_2, with statistical significance in parentheses.
* Probability for the overall correlation.

We also examined the Pearson correlation coefficient (r) between N_I and N_B. For the data set as a whole ($n = 33$; outlier from N_B population excluded), the two types of pore densities correlated with each other ($r = 0.47$; $P < 0.01$). For the data subsets (PM < 15, 20, or 25 hours), no statistically significant correlation was found ($P > 0.15$).

No statistically significant correlations were found between age and N_I ($P > 0.07$) or N_B ($P > 0.04$, outlier excluded), although P approached statistical significance. When data from both 5-year-old eyes were excluded, P was much higher ($P > 0.14$ and $P > 0.2$, respectively). Figure 5 shows pore density as a function of age for the adult eyes.

Pore Sizes

With the major axis of the pore as the pore diameter, D_I was 0.97 ± 0.23 μm ($n = 34$; mean ± SD) and D_B was 1.64 ± 0.36 μm ($n = 34$); with the geometric mean of the major and minor axes of the pore as the pore diameter, D_I was 0.75 ± 0.19 μm ($n = 34$) and D_B was 1.13 ± 0.26 μm ($n = 34$). We also examined the correlation between the diameter of the pores and the other variables. The only statistically significant correlation was between the pore size of the intracellular pores and that of the border pores (whole data set: $r = 0.48$, $P < 0.005$, $n = 34$; PM < 25 hours: $r = 0.59$, $P < 0.01$, $n = 19$).

Outflow Facility

Prefixation C correlated with patient age and with fixation pressure, as previously reported.[16] Similarly, outflow facility after fixation correlated with patient age. Including the pore density and pore diameters of the intracellular pores and border pores with these correlations showed one further correlation:

$$C = d_0 + d_1{*}\text{IOP} + d_2{*}\text{Age} + d_3{*}D_B \quad (4)$$

with the coefficients shown in Table 6. D_B in Equation 4 is based on the pore major axis; a similar, but statistically less significant result ($P < 0.02$ for d_3), was found using the mean pore diameter (see Methods section). A statistically significant correlation was found only for the data set as a whole, and no such correlation (involving pore densities or diameters) was found for the data subsets involving shorter PM ($P > 0.5$).

Several theories have been proposed to relate the number and size of the pores of the inner-wall endothelium to the flow resistance generated by this cell layer. These include Poiseuille's law,[7] Sampson's law,[7] and the theory of funneling,[20] which predict a scaling relationship of C with pore number and size as $N \cdot D^4$, $N \cdot D^3$, and $N \cdot D$, respectively. When excluding the single outlier for D_B (see earlier explanation), no correlation was found between C and any of these combinations in intracellular pores ($P > 0.4$) or in border pores ($P > 0.1$).

DISCUSSION

Pores passing through the inner-wall endothelium of Schlemm's canal were first identified by Holmberg.[4] These pores usually were associated with giant vacuoles but also were seen occasionally in flat regions of the inner wall.[6] Using scanning EM (Fig. 1), we have found that the inner-wall endothelium has two distinct types of pores: an intracellular pore population (pores passing through the inner wall endothelial cells) and an intercellular (or border) pore population (pores passing between the cells). In primate eyes, Epstein and Rohen[17] identified a pathway between inner-wall endothelial cells through which an undetermined fraction of aqueous humor passes, and we postulate that the intercellular pores seen in our study corresponded to the luminal opening of the paracellular pathway identified by Epstein and Rohen.

The major conclusion of the present study is that the two pore types show markedly different dependencies on important experimental parameters, such as IOP, V_F, and PM. In particular, we found that the intracellular pore density was

TABLE 4. Coefficients for Equation 2

Postmortem Time (h)	n	b_0	b_1	b_2	P^*
All data	34	1830 ± 270	−43.2 ($P < 0.001$)	NS ($P = 0.48$)	<0.001
<25 hours	19	1870 ± 320	−77.1 ($P < 0.001$)	2.72 ($P < 0.01$)	<0.001
<20 hours	14	1750 ± 350	−91.1 ($P < 0.001$)	4.80 ($P < 0.0005$)	<0.00002
<15 hours	9	540 ± 230	NS ($P = 0.090$)	5.77 ($P < 0.005$)	<0.005

NS, not significant at $P = 0.01$. Values for b_0 are means ± SE and means for b_1 and b_2, with statistical significance in parentheses.
* Probability for the overall correlation.

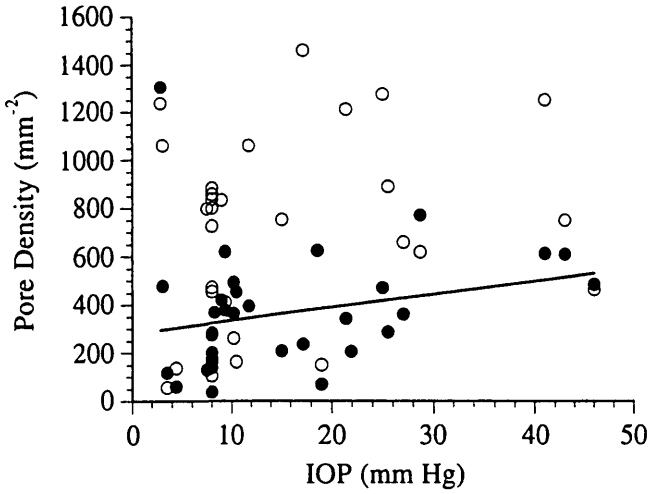

FIGURE 4. Pore density as a function of fixation pressure. (○), intracellular pores; (●), border pores. The *solid line* is the best linear fit to the border pore data ($P < 0.005$). No correlation was found between intracellular pore density and fixation pressure ($P > 0.4$).

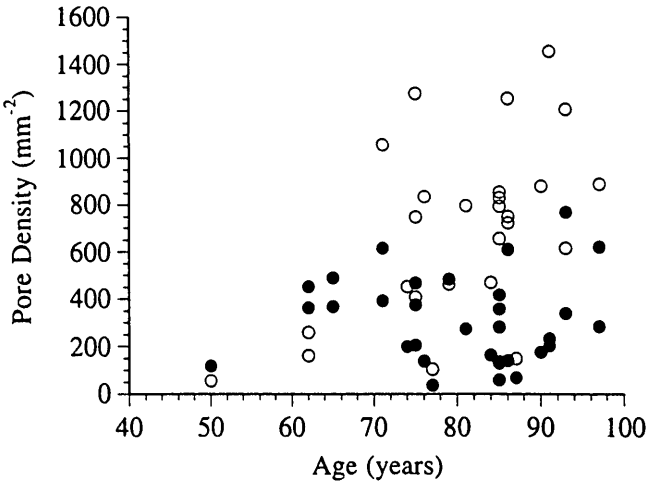

FIGURE 5. Pore density as a function of age for adult eyes. (○), intracellular pores; (●), border pores. No correlation was found between age and intracellular pore density ($P > 0.2$) or border pore density ($P > 0.14$).

observed to decrease with PM and to increase with the V_F (Eq. 1); in contrast, N_B did not depend on these parameters, but instead increased with IOP (Eq. 3). Thus, these two types of pores seem to be functionally and morphologically distinct.

The dependence of N_I on PM and total V_F and the absence of dependence on flow-related variables such as IOP and V_F suggests that intracellular pores may be fixation artifacts. Similar logic may suggest that border pores are not fixation artifacts. However, at present, it is impossible to conclude definitively that either one (or both) pore types are artifacts. If intracellular pores were artifacts not present in vivo, a calculation using the methodology of Bill and Svedbergh[7] indicates that border pores would generate most of the known aqueous outflow resistance. Clearly, determination of the actual in vivo pore distribution in the inner wall of Schlemm's canal is required.

How PM and V_F affect intracellular pores and how fixation pressure affects border pores is unclear. We have previously hypothesized[16] that the effect of PM on pore density may be caused by loss of inner-wall endothelial cell viability, thus decreasing the cellular capability to form pores. The effect of V_F was attributed to pores continuing to form during the fixation process; thus, rather than a "snapshot" of the inner wall, a "time exposure" image was seen. The increase in D_B with increasing IOP may have been caused by increased stress on the intercellular junctions, promoting pore formation. To investigate these hypotheses, improved methods of studying the inner wall may be required. It is interesting that pore density and the pore diameter of the intercellular and border pores correlated with each other (at least for the longer PM), which suggests that there may be some interaction between the pore types. However, the nature of this interaction (if any) is unclear at present.

We have previously proposed[20] that a hydrodynamic interaction between the pores in the inner-wall endothelium and the juxtacanalicular connective tissue could lead to an enhanced effective flow resistance of the juxtacanalicular region (the funneling effect). Other theories of how inner-wall pores may influence outflow facility have also been proposed: short pores passing through an otherwise impermeable inner wall[7] (inner-wall flow resistance given by Sampson's law), and long pores[7] (inner-wall flow resistance given by Poiseuille's law). Each of these theories predicts relationships between outflow facility and inner-wall pore characteristics.

However, when we previously used data for all pores,[16] we did not find support for any of these predicted relationships. The present study also found no such correlations, considering either the intracellular pores or for the border pores individually. In the case of Sampson's law or Poiseuille's law, in which the pores are themselves entirely responsible for generating flow resistance, this absence of correlation argues strongly against inner-wall pores playing a major role in determining flow resistance. However, in the case of the funneling theory, such a conclusion is less clear cut, because aqueous outflow resistance in that case is primarily determined by the hydraulic conductivity of the extracellular matrix in the juxtacanalicular connective tissue, and pores act only to modulate flow resistance in the juxtacanalicular connective tissue. For this reason, a strong statistical correlation between outflow facility and inner-wall pore characteristics may be difficult to obtain, without also determining the hydraulic conductivity of the juxtacanalicular connective tissue.

In this discussion, we have implicitly assumed that the pores are short straight-through openings in the inner wall of Schlemm's canal. Under high magnification, it is possible to see

TABLE 5. Coefficients for Equation 3

Postmortem Time (h)	n	c_0	c_1
All data	33	200 ± 50	8.64 ($P < 0.005$)
<25 hours	18	360 ± 50	NS ($P = 0.035$)
<20 hours	14	370 ± 60	NS ($P = 0.031$)
<15 hours	9	410 ± 60	NS ($P = 0.164$)

NS, not significant at $P = 0.01$. Values for d_0 are means ± SE and means for d_1 and d_2, with statistical significance for the overall correlation in parentheses.

TABLE 6. Coefficients for Equation 4

Postmortem Time (h)	n	d_0	d_1	d_2	d_3	P^*
All data	34	0.502 ± 0.076	−0.00396 ($P < 0.01$)	−0.00585 ($P < 10^{-8}$)	0.124 ($P < 0.005$)	$<10^{-9}$

Values for d_0 is means ± SE and means for d_1, d_2, and d_3, with statistical significance in parentheses.
* Probability for the overall correlation.

an amorphous porous material through the mouth of some of the larger pores. Such material is probably juxtacanalicular tissue, and this would seem to support the assumption that the pores are short passages. However, in their study of paracellular pores, Epstein and Rohen[17] noted that some intercellular pores can be long and tortuous, eventually enlarging at their opening to the lumen of Schlemm's canal. If our border pores correspond to these paracellular pathways, it is possible that the structure that we see as a pore in the inner-wall endothelium may not entirely reflect the geometry and flow resistance of the underlying flow channel. If this were the case, it would require further rethinking of our concept of a "pore" in the context of Schlemm's canal, and could explain the absence of correlation between outflow facility and the predictions of the hydrodynamic models investigated.

A current controversy regarding microvascular hydraulic permeability also involves two types of endothelial pores (or "gaps" in their terminology): those passing between the cells and those passing through the cells. Although it is widely believed that microvascular permeability is controlled by the intercellular pathway, Neal and Michel[21] have shown that when an ionophore is used to increase microvascular permeability, this increase is associated with an increased number of intracellular pores, with little or no change in the intercellular pathway. These changes in permeability and pore number were reversed by perfusion with ionophore-free solutions. It is possible that the two types of pores we have investigated in the inner-wall endothelium of Schlemm's canal are related to those involved in fluid transport across the vascular endothelium.

Summarizing, we have found two types of pores in the inner-wall endothelium that correlate very differently with fixation parameters. Further study, probably using new techniques that show better the in vivo state of the inner-wall of Schlemm's canal, is needed to determine what role these two types of pores play in influencing outflow facility.

References

1. Grant WM. Clinical measurements of aqueous outflow. *Arch Ophthalmol.* 1951;46:113-131.
2. Seidel E. Experimentelle Untersuchungen uber die Quelle und den Verlauf der intracoluaren Saftstromung. *Graefes Arch Clin Exp Ophthalmol.* 1918;95:1.
3. Garron LK, Fenney ML, Hogan MJ McEwen WK. Electron microscopic studies of the human eye. *Am J Ophthalmol.* 1958;40:27-35.
4. Holmberg A. The fine structure of the inner wall of Schlemm's canal. *Arch Ophthalmol.* 1959;62:956-958.
5. Tripathi RC. Ultrastructure of Schlemm's canal in relation to aqueous outflow. *Exp Eye Res.* 1968;7:335-341.
6. Inomata H, Bill A, Smelser GK. Aqueous humor pathways through the trabecular meshwork and into Schlemm's canal in cynomologus monkey (Macca Irus). *Am J Ophthalmol.* 1972;73:760-789.
7. Bill A, Svedbergh B. Scanning electron microscopic studies of the trabecular meshwork and the canal of Schlemm: an attempt to localize the main resistance to outflow of aqueous humor in man. *Acta Ophthalmol.* 1972;50:295-320.
8. Moseley H, Grierson I, Lee WR. Mathematical modelling of aqueous humor outflow from the eye through the pores in the lining of Schlemm's canal. *Clin Phys Physiol Meas.* 1983;4:47-63.
9. Grierson I, Lee WR, Mosley H, Abraham S. The trabecular wall of Schlemm's canal: a study of the effects of pilocarpine by scanning electron microscopy. *Br J Ophthalmol.* 1979;63:9-16.
10. Ethier CR, Kamm RD, Palaszewski BA, Johnson MC, Richardson TM. Calculations of flow resistance in the juxtacanalicular meshwork. *Invest Ophthalmol Vis Sci.* 1986;27:1741-1750.
11. Alexander JP, Samples JR, Van Burkirk EM, Acott TS. Expression of matrix metalloproteinases and inhibitor by human trabecular meshwork. *Invest Ophthalmol Vis Sci.* 1991;32:172-180.
12. Seiler T, Wollensak J. The resistance of the trabecular meshwork to aqueous humor outflow. *Graefes Arch Clin Exp Ophthalmol.* 1985;223:88-91.
13. Maepea O, Bill A. Pressures in the juxtacanalicular tissue and Schlemm's canal in monkeys. *Exp Eye Res.* 1992;54:879-883.
14. Hamanaka T, Bill A. Morphological and functional effects of Na2EDTA on the outflow routes for aqueous humor in monkeys. *Exp Eye Res.* 1987;44:171-190.
15. Hamanaka T, Bill A. Effects of alpha-chymotrypsin on the outflow routes for aqueous humor. *Exp Eye Res.* 1988;46:323-341.
16. Sit AJ, Coloma FM, Ethier CR, Johnson M. Factors affecting the pores of the inner-wall endothelium of Schlemm's canal. *Invest Ophthalmol Vis Sci.* 1997;38:1517-1525.
17. Epstein DL, Rohen JW. Morphology of the trabecular meshwork and inner-wall endothelium after cationized ferritin perfusion in the monkey eye. *Invest Ophthalmol Vis Sci.* 1991;32:160-171.
18. Weisberg S. *Applied Linear Regression.* New York: John Wiley & Sons; 1985:114-121.
19. Glynn RJ, Rosner B. Accounting for the correlation between fellow eyes in regression analysis. *Arch Ophthalmol.* 1992;110:381-387.
20. Johnson M, Shapiro A, Ethier CR, Kamm RD. Modulation of outflow resistance by the pores of the inner-wall endothelium. *Invest Ophthalmol Vis Sci.* 1992;33:1670-1675.
21. Neal CR, Michel CC. Trancellular gaps in microvascular walls of frogs and rat when permeability is increased by perfusion with the ionophore A23187. *J Physiol.* 1995;488:427-437.